

Computer Simulations of the Static Scattering from Model Polymer Blends

S. T. Cui,^{†,‡} H. D. Cochran,^{†,‡} P. T. Cummings,^{†,‡} and S. K. Kumar^{*,§}

Department of Chemical Engineering, University of Tennessee, Knoxville, Tennessee 37996-2200, Chemical Technology Division, Oak Ridge National Laboratory, P.O. Box 2008, Building 4500N, Oak Ridge, Tennessee 37831, and Department of Materials Science and Engineering, The Pennsylvania State University, University Park, Pennsylvania 16802

Received July 12, 1996; Revised Manuscript Received November 25, 1996[®]

ABSTRACT: To understand the unusual composition and wave vector, q , dependent Flory interaction parameters, χ , obtained from small angle neutron scattering (SANS), we have calculated the three partial structure factors for symmetric binary polymer blends with relatively strong interactions between dissimilar monomers using molecular dynamics simulations. In agreement with past work we find that the radii of gyration of the chains are altered on blending. The following new results emerged from our simulations. The single-chain form factors in the blends follow Gaussian statistics at all distances larger than a monomer diameter, confirming the Flory–de Gennes conjecture that correlations in condensed polymer phases are screened over short length scales. The R_g 's deduced from these form factors are in agreement with simulation-determined values and illustrate conclusively that the single chain term in the incompressible random-phase approximation (i-RPA) is altered on blending. The three partial structure factors obtained from the simulations, each of which follows an Ornstein–Zernike behavior, have different q dependences and extrapolate to different values in the thermodynamic limit. The different q dependences can be explained qualitatively by a compressible RPA formalism proposed by Tang and Freed. We then show that any form chosen to combine these partial structure factors into a single total scattering function will, in general, not have a q dependence that is describable by the incompressible RPA. This explains the experimentally observed q dependence of the χ parameter derived from the i-RPA. Finally, a thermodynamic analysis on the zero wave-vector limit of the partial structure factors shows that their absolute values are different from each other due to the effects of density fluctuations, as well as the different partial molar volumes of the two species in the blend. These results serve to emphasize the important role played by compressibility on the scattering obtained from simple polymer mixtures with large excess volumes on mixing.

1. Introduction

There is considerable interest in polymeric materials due to their importance in industrial and everyday applications. It is often advantageous to blend two or more polymers¹ since this can result in materials with highly controllable physical properties. One major challenge in this approach is the incompatibility which can arise from mixing two polymers. In this context a widely used theory for describing the phase behavior of polymer blends is the incompressible lattice-based Flory–Huggins model.² This theory predicts that the free energy of mixing for a binary polymer blend is

$$\frac{\Delta G}{k_B T} = \frac{\phi_1}{N_1} \ln \phi_1 + \frac{\phi_2}{N_2} \ln \phi_2 + \chi \phi_1 \phi_2 \quad (1)$$

where ΔG is the free energy of mixing per lattice site, k_B is Boltzmann's constant, T is the temperature, N_i is the degree of polymerization of component i , and ϕ_i is the corresponding volume fraction. If the system followed the assumptions built into Flory theory, then the interchange energy parameter, χ , could be determined from small-angle neutron scattering (SANS) experiments using the incompressible random-phase approximation (i-RPA),³ which is the scattering analog of Flory theory:

$$\frac{1}{S(q)} = \frac{1}{N_1 \phi_1 P_1(qR_{g1})} + \frac{1}{N_2 \phi_2 P_2(qR_{g2})} - 2\chi \quad (2)$$

Here $S(q)$ is the static structure factor of the blend, $P_i(qR_{gi})$ and R_{gi} are the form factor and the radius of gyration, respectively, of component i , and q is the wave vector. Consistent with Flory theory, in the i-RPA model, chains assume their unperturbed Gaussian dimensions in the pure state and in the blend. Further, the χ parameter is assumed to be a system-specific constant that only depends on temperature.

In contrast to these theoretical ideas, recent experiments^{4–7} have found that the SANS-determined χ parameters for a number of polymer blends are composition dependent, and in some cases molecular weight and wave-vector dependent. While a large amount of theoretical and experimental research^{8–19} has been devoted to this subject, the molecular origin of these effects remains unresolved at this time. From a theoretical viewpoint it has been suggested that one of the following factors, which have been ignored in the incompressible Flory–Huggins model, must be the underlying cause of the observed composition, molecular weight, and wave-vector dependence of the χ parameter:

1. Muthukumar⁸ and Olvera et al.⁹ have suggested that concentration fluctuation effects, which are present in any polymer mixture but are not accounted for in a mean-field model, such as Flory's, can help to rationalize the observed experimental trends.

2. Freed,¹⁰ Sanchez,¹⁴ and Taylor et al.¹⁵ have argued that the finite but nonzero compressibility of a polymeric system has to be incorporated to properly capture the

[†] University of Tennessee.

[‡] Oak Ridge National Laboratory.

[§] The Pennsylvania State University.

[®] Abstract published in *Advance ACS Abstracts*, May 1, 1997.

observed dependences of the SANS-determined interaction parameter.

3. Schweizer and his co-workers¹¹ have suggested that liquid-state-like packing effects, which are ignored in any model that assumes the random mixing of chain segments, must play a vital role in determining the composition and wave-vector dependence of the SANS-derived χ parameter.

While it is unclear which of these different factors is critical to understanding the scattering from polymer mixtures, we stress that computer simulations are particularly relevant since they can delineate the various molecular factors which underlie experimental behavior. To our knowledge, there are two different sets of simulation data which have attempted to address the scattering that is obtained from a polymer blend system and hence the dependences of the SANS-derived interaction parameter. Below we summarize these findings:

1. Binder and his co-workers^{17–19} have calculated the collective structure factors for binary blends of short chains ($N = 16$ and 32 , respectively). They found some evidence for the composition dependence of the SANS-derived χ parameter. However, this work employed several simplifications which could affect the results obtained. First, the chain lengths employed are relatively short. Second, the quantity which is calculated in these simulations is a collective structure factor.¹⁹ In contrast, the experimentally determined structure factor is a measure of the three relevant partial structure factors weighted by the appropriate scattering lengths. Consequently, material-specific constants (such as the neutron contrast factor) explicitly affect the measured value of the blend structure factor. While all of these structure factors have the same information content in the limit of an incompressible system, the same is not true in the case of a system with finite compressibility. The relationship of the structure factors determined from the simulations of Binder and the experimentally measured quantities is therefore unclear. Due to these factors there is a need to reexamine the calculation of blend scattering in the context of a computer simulation.

2. Kumar¹⁵ has utilized computer simulations to derive the chemical potentials of the two components of a binary polymer blend. The partial structure factors of the blends can then be deduced from this information through the use of standard relationships.¹⁵ While this work is able to shed some light on the observed variation of the χ parameter with state variables, it is clear that the calculation of structure factors from simulation-derived chemical potentials is indirect. Further, this work cannot comment on the observed wave-vector dependences since it has only focused on the zero wave-vector, or thermodynamic, limit.

While there has, therefore, been considerable simulation work present in the literature, these do not explicitly address the various factors controlling the observed complicated behavior of the SANS-derived χ parameters. To resolve some of these issues, here, we have carried out simulations using essentially the same polymer mixture model as Kumar's but have also considered higher densities and longer chains. We have compared results obtained at three different compositions at each density and have considered three separate densities in a series of simulations. The simulations were performed on the massively parallel Intel Paragon supercomputers located at the Oak Ridge National Laboratory. A domain decomposition technique for

chain systems was used for this simulation as discussed elsewhere.²⁰ While the simulation of polymer blends is an extremely popular research topic today, we have focused explicitly on understanding the scattering obtained from a model mixture. The following novel features, which were obtained from our simulations, will be stressed in this paper:

1. We explicitly calculate the three partial structure factors of the polymer blend. This permits us to comment directly on the scattering obtained from a polymer blend. To obtain a detailed understanding of the various factors which cause the state dependence of the SANS-determined χ parameter, we shall examine all of the assumptions made in deriving the i-RPA.

2. We begin by considering the single-chain structure (or form) factors of the two components in the blend, $P(qR_g)$ (see eq 2). We found that these quantities in the blends were describable over a relatively large q range by Gaussian statistic, but with the simulation-derived values of the radii of gyration at that state condition. This verifies the commonly accepted result that correlations in a melt are screened over relatively short distances. However, we found, in agreement with experiment¹⁶ and past simulations,^{15,17–20} that the R_g 's for the two components were altered on blending.

3. Since we have a direct knowledge of the various form factors, we proceeded to calculate the three partial structure factors. We found that each followed Ornstein–Zernike behavior, but with different q -dependences and zero wave-vector limits. Since this behavior is not caused by inaccuracies in modeling the form factors, consequently, we conjecture that the different q -dependences are a consequence of compressibility effects, which can be captured qualitatively by a compressible RPA formalism.¹⁰ When these partial structure factors are combined into a single structure factor, in general, the q -dependence of the resulting function cannot be described by the incompressible RPA formalism. Consequently, the χ parameter resulting from the i-RPA after one uses eq 2 has a linear dependence on q^2 , in qualitative agreement with experiment.

4. Finally, we employed a thermodynamic analysis to understand the role played by compressibility in the zero wave-vector limit. On the basis of our findings, we conclude that it is inappropriate to model SANS data from polymer blends through the use of the i-RPA formula and that the Flory description of blend thermodynamics might be oversimplified even in the context of these highly idealized mixtures.

These issues will be discussed below in more detail.

2. Model and Simulation Method

We studied two binary symmetric polymer blends comprised of chain lengths 25 and 50 monomers, respectively. The systems consisted of 13 500 monomers in all cases. This relatively large system is required since the structure factors need to be determined at small wave vector, q , so as to facilitate the extrapolation to the thermodynamic limit, $q = 0$. The monomers in a chain are connected by a finite extensible nonelastic spring potential

$$u_{ij} = \begin{cases} -0.5kR_0^2 \ln[1 - (r_{ij}/R_0)^2], & r_{ij} \leq R_0 \\ \infty, & r_{ij} \geq R_0 \end{cases} \quad (3)$$

where r_{ij} is the distance between two neighboring monomers, and the parameters k and R_0 are 50ϵ and 1.4σ , respectively. These values are close to those used

by Kremer and Grest²¹ (i.e., $k = 30\epsilon$, $R_0 = 1.5\sigma$). We have chosen slightly different parameters to ensure that the chains do not cross each other at the higher temperatures employed in this work. In addition, all monomers interact with a shifted force Lennard-Jones potential with a cutoff distance $r_c = 2.5\sigma$. The form of the potential ensures that the potential and its derivative, the negative of the force, continuously approach zero at r_c .²⁴

$$v_{\text{SF}}^{ab}(r_{ij}) = \begin{cases} v^{ab}(r_{ij}) - v_c^{ab} - \left(\frac{dv^{ab}(r_{ij})}{dr_{ij}} \right)_{r_{ij}=r_c} (r_{ij} - r_c) & r_{ij} \leq r_c \\ 0, & r_{ij} > r_c \end{cases} \quad (4)$$

$v^{ab}(r_{ij})$ is the Lennard-Jones potential between particles of species a and b ,

$$v^{ab}(r_{ij}) = 4\epsilon_{ab} \left[\left(\frac{\sigma_{ab}}{r_{ij}} \right)^{12} - \left(\frac{\sigma_{ab}}{r_{ij}} \right)^6 \right] \quad (5)$$

ϵ_{ab} and σ_{ab} are the energy and length parameters, respectively, r_{ij} is the distance between monomers i and j , and v_c is the value of the Lennard-Jones potential at the cutoff distance. In this work we have studied symmetric blends where both chains are of identical length, N , and identical monomer sizes, σ . The Lennard-Jones energy parameters for similar pairs of beads were identical, i.e., $\epsilon_{aa} = \epsilon_{bb} = \epsilon$, but the energy of interaction between dissimilar pairs is different. Two different classes of blends were studied in this work. One is an attractive blend, in which $\epsilon_{ab} = 1.2\epsilon$, $T^* = k_B T/\epsilon = 2.0$, and $N = 25$. The system was studied at three reduced monomer densities, $\rho^* = \rho\sigma^3 = 0.70, 0.80$, and 0.85 , respectively. Three different compositions, $\phi = 0.1, 0.25$, and 0.50 , were considered at each density. The lowest density case was that studied by Kumar.¹⁵ The other system we studied was a repulsive blend, in which $\epsilon_{ab} = 0.99\epsilon$, $T^* = 1.5$, and $N = 50$. The density for this system was $\rho^* = 0.70$, and the compositions are $\phi = 0.1, 0.25$, and 0.50 , respectively. Note that in the case of the repulsive system we do not consider smaller values of ϵ_{ab} since blends comprised of chains of length $N = 50$ tend to phase separate under these conditions. However, the repulsive blend considered in this work is miscible under the conditions examined.

The initial configurations of the systems were generated using a continuum configurational bias²² (CCB) Monte Carlo scheme, which efficiently generated a spatially uniform total monomer density distribution. For $N = 25$, chains in this initial state had essentially their equilibrium radius of gyration. However, for $N = 50$, the average initial radius of gyration of the polymer molecules was different from its equilibrium value. For $N = 25$ and $\rho^* = 0.70$, a constant-temperature molecular dynamics simulation was run for a time of $2.5 \times 10^3\tau$ for equilibration, where $\tau = (m\sigma^2/\epsilon)^{1/2}$, and m is the monomer mass. Each time step was 0.005τ . For $N = 25$ and $\rho^* = 0.80$ and 0.85 , the equilibration time was $5 \times 10^3\tau$. For the longer chain ($N = 50$), we equilibrated the system for $1.5 \times 10^4\tau$. According to the Rouse model,²³ the longest relaxation time τ_N for a chain is given by

$$\tau_N = \frac{\langle R^2(N) \rangle}{3\pi^2 D} \quad (6)$$

Table 1. State Points and Production Run Lengths

ρ^*	T^*	N	$\tau_{\text{tot}} (10^3\tau)$		
			$\phi = 0.10$	$\phi = 0.25$	$\phi = 0.50$
0.70	2.0	25	22.3	25.5	25.6
0.80	2.0	25	23.5	25.0	23.6
0.85	2.0	25	35.1	27.5	21.7
0.70	1.5	50	42.4	40.9	63.3

where D is the diffusion constant and $\langle R^2(N) \rangle$ is the mean squared end-to-end distance of the polymer chain consisting of N monomers. Based on the values of D and $\langle R^2(N) \rangle$ calculated in previous work,²¹ τ_N was estimated to be 580τ for $N = 25$ and $3.5 \times 10^3\tau$ for $N = 50$, respectively, at $\rho^* = 0.85$. At all densities our equilibration times are larger than these estimates.

During the equilibration step, we have used Kremer and Grest's equations of motion²¹ to update the position and velocity. The integration scheme for the equilibration was standard Brownian dynamics.²⁴ A reduced time step size of 0.005τ was used. After equilibration, the thermostat was turned off, and the system was allowed to evolve following Newton's equations of motion in a constant energy simulation. Since the system had been sufficiently equilibrated, the average temperature of the system in the constant energy simulation was within 1.5% of the preset temperature. The production run length for each state condition is tabulated in Table 1.

3. Results and Discussion

3.1. Single Chain Properties. We begin by examining the single-chain form factors, $P(qR_g)$, which are related to single-chain conformations and play a central role in the i-RPA (eq 2). To our knowledge, no one has examined this issue, and, consequently, our findings should shed considerable light on the use of this quantity in eq 2. $P(q)$ is defined as

$$P(q) = \frac{1}{N^2} \left\langle \left| \sum_{i=1}^N \exp(iq \cdot \mathbf{r}_i) \right|^2 \right\rangle \quad (7)$$

which is equivalent to the single-chain structure factor apart from a factor of $1/N$, and \mathbf{r}_i is the position of monomer i in a chain molecule. Since our model chains are fully flexible, we expect them to obey Gaussian chain statistics to a reasonable approximation. Thus, $P(q)$ should be describable, apart from a factor N , by the Debye function.²⁵ The form factors from the simulation are shown in parts a and b of Figure 1 at a density $\rho^* = 0.70$ for $N = 25$ and $N = 50$ and $\phi = 0.5$. To obtain the theoretically predicted form factors, we need to know the radii of gyration, $\langle R_g^2 \rangle^{1/2}$, of the chains. To obtain this quantity, we replot the form factors as $1/P(q)$ vs q^2 . This yields a near straight line as can be observed in Figure 2. The data are best fit by a quadratic, and the coefficient of the linear term is equal to $\langle R_g^2 \rangle/3$. The R_g values (in this paper, we use σ as the units for the radius of gyration unless otherwise noted) obtained from this procedure are compared to the radius of gyration obtained directly from the simulations in Table 2. Several issues are clear here. First, the radii of gyration obtained by both methods are in excellent agreement, suggesting that the single-chain structure in these blends is described well, at low q , by a Gaussian form. This point is illustrated clearly in Figure 1, where the Debye functions, using the radii of gyration in Table 2, are superposed on the form factors. The theoretical predictions accurately determine the single-chain struc-

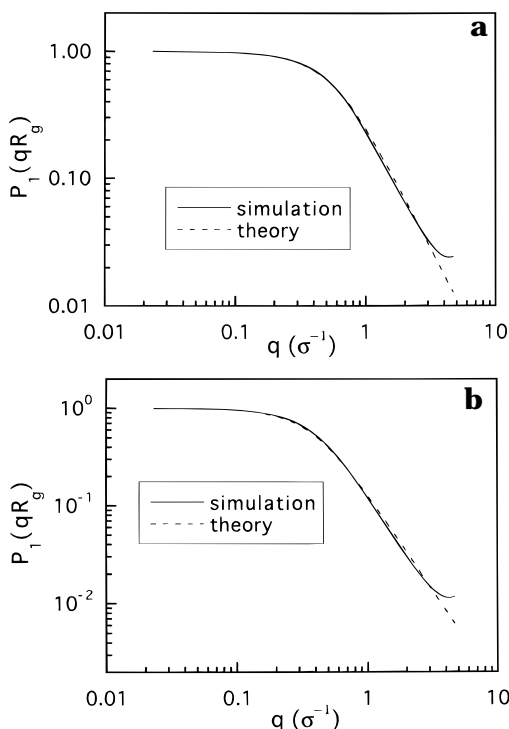


Figure 1. (a) Form factor of a $N = 25$ chain of component 1 (the minority component) at composition $\phi = 0.50$ and $\rho^* = 0.70$. The solid line is the simulation result and the dashed line is the Debye function using the radius of gyration $\langle R_g^2 \rangle^{1/2} = 2.57\sigma$ calculated from the simulation. (b) Form factor of a $N = 50$ chain of component 1 at composition $\phi = 0.50$ and $\rho^* = 0.70$. The symbols are the same as in part a. $\langle R_g^2 \rangle^{1/2} = 3.63\sigma$ was used in calculating the Debye function.

ture factor, especially at low wave vector. At large wave vector ($q^* = q\sigma > 3.0$), the Debye function strongly deviates from the simulation result. Since this occurs at distances [i.e., $r^* \approx \pi/q^* = \pi/(q\sigma)$] smaller than 1, this verifies the Flory-de Gennes²⁶ conjecture that correlations in the melt are screened at distances comparable to the monomer size. Essentially the same behavior was observed under all conditions simulated. It is, therefore, clear that the i-RPA assumption of Gaussian chain statistics is valid at the level of the form factors. Consequently, the state dependence of the SANS-derived interaction parameter is not caused by discrepancies in this quantity.

A second fact that emerges from Figure 2 is that the minority component in the blend undergoes an expansion or contraction. This result appears to be well-known from experiment, simulation, and theory. The radius of gyration of the minority chains increases by about 5% at the extreme composition for the attractive mixture. For the repulsive mixture, as the composition of component 1 decreases, its radius of gyration decreases about 1%. Here we note that the difference in the interaction strength (the Lennard-Jones energy parameter) between the different species in the repulsive mixture is 1%, while it is 20% in the case of the attractive mixture. This suggests that, for real polymer systems where the differences are likely to be on the order of 1%, the chain expansion (or contraction) effect should be small. This result is in agreement with experiments.¹⁶

3.2. Structure Factor and the χ Parameter. We shall now proceed to examine the behavior of the partial structure factors, $S_{ij}(0)$, and hence the total structure factor. As noted above, the experimental combination

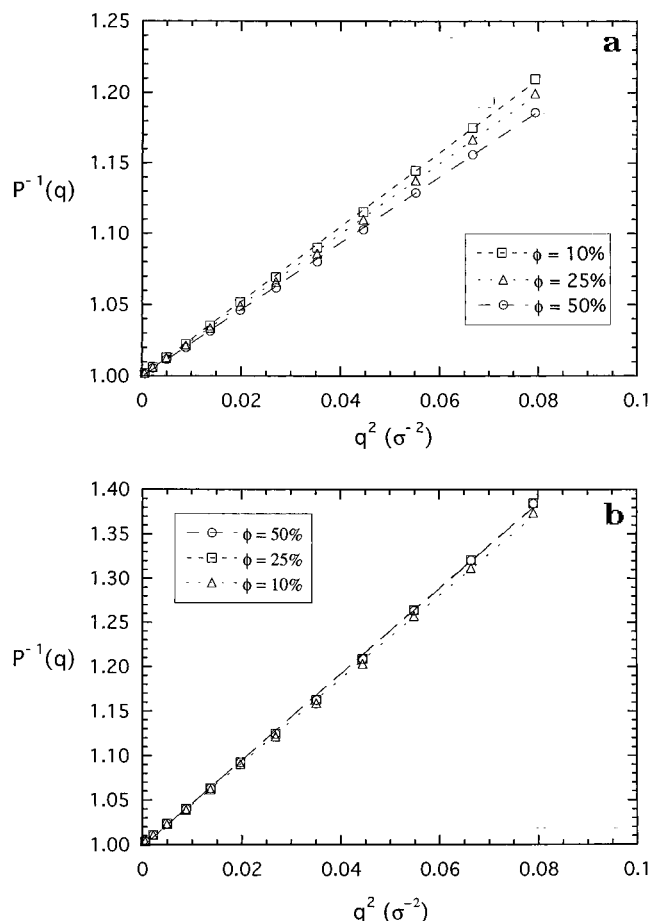


Figure 2. (a) Zimm plot of the single-chain form factor for component 1 with chain length $N = 25$ at $\rho^* = 0.70$, at three different compositions, $\phi = 0.1, 0.25$, and 0.50 . The data for each composition were fitted to a quadratic function. The radius of gyration can be obtained from the coefficient of the linear term in q^2 , α , from the relation $\langle R_g^2 \rangle/3 = \alpha$. (b) Similar to part a, but for chain length $N = 50$. The blend is a repulsive mixture.

Table 2. Radii of Gyration for Chains of Component 1 in the Blends at Various State Conditions^a

ρ^*	T^*	N	$\langle R_g^2 \rangle^{1/2} b$		
			$\phi = 0.10$	$\phi = 0.25$	$\phi = 0.50$
0.70	2.0	25	2.70 (2)	2.65 (1)	2.57 (1)
			2.73	2.67	2.58
0.80	2.0	25	2.72 (1)	2.64 (1)	2.55 (1)
0.85	2.0	25	2.72 (1)	2.63 (1)	2.53 (1)
0.70	1.5	50	3.59 (1)	3.63 (1)	3.63 (1)
			3.60	3.64	3.64

^a The numbers in the parentheses represent statistical uncertainty. Consequently 2.70 (2) implies 2.70 ± 0.02 . The first three sets of data refer to the attractive $N = 25$ system, while the last set of data corresponds to the repulsive $N = 50$ blend. ^b The first row in the radius of gyration at the number density $\rho^* = 0.70$ was obtained from direct calculation, the second row was obtained from fitting the single-chain structure factor to a quadratic function of q^2 . Note that although it is difficult to estimate the uncertainties in $\langle R_g^2 \rangle^{1/2}$ obtained from curve fitting, the goodness of the curve fitting suggests that the errors are small.

of the three partial structure factors into a total structure factor has to incorporate material-specific quantities such as scattering lengths. To avoid the use of arbitrary constants and also to draw more general conclusions, we shall follow a method suggested earlier by Schweizer.¹¹ However, it is important to stress that our conclusions are robust and are not affected by this approximation. To illustrate our methodology for the

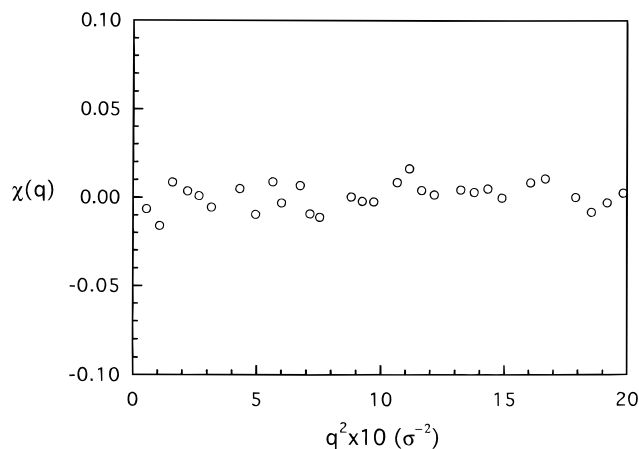


Figure 3. Calculated χ parameter as a function of q^2 for the ideal blend, where q is the wave vector.

calculation of χ from the three partial structure factors obtained from the simulations, we begin by studying an idealized system comprised of chains of length $N = 25$ where *all* monomers interact with the same potential. We artificially divide the system into two components with equimolar composition and calculate the partial structure factors. For computational efficiency, the Lennard-Jones interaction between monomers is replaced by a WCA (Weeks–Chandler–Andersen) potential,²⁴ i.e.

$$v_{\text{wca}}(r_{ij}) = \begin{cases} 4\epsilon \left[\left(\frac{\sigma}{r_{ij}} \right)^{12} - \left(\frac{\sigma}{r_{ij}} \right)^6 + \frac{1}{4} \right], & r_{ij} \leq 2^{1/6}\sigma \\ 0, & r_{ij} > 2^{1/6}\sigma \end{cases} \quad (8)$$

In this case the system will, by construction, satisfy the criterion $S_{11}(q) = S_{22}(q) = -S_{12}(q)$. We now need a method for combining the three partial structure factors into a single total structure factor for the blend. We follow the recent suggestion by Schweizer¹¹ and use

$$\frac{4}{S(q)} = \frac{1}{S_{11}(q)} + \frac{1}{S_{22}(q)} - \frac{2}{S_{12}(q)} \quad (9)$$

The χ parameter is then derived from $S(q)$ utilizing the i-RPA (eq 2), with a knowledge of the single-chain form factors. In Figure 3, we plot the χ parameter at $\rho^* = 0.70$ and $T^* = 2$ as a function of q^2 for this idealized system. As expected, $\chi \approx 0$ independent of q as shown in the figure. We, therefore, conclude that this methodology for the calculation of interaction parameters from partial structure factors through the device of the incompressible RPA model provides reasonable results.

The χ values for the attractive $N = 25$ system calculated in the same fashion are presented in parts a–c of Figure 4, where we plot $\chi(q)$ as a function of q^2 at $\rho^* = 0.70, 0.80$, and 0.85 , respectively. Note that we have employed the form factors obtained from the *blend* simulations to define the ideal chain scattering in eq 2. These figures clearly show that χ varies linearly with q^2 even at low q , apparently in good agreement with experimental results obtained on polyolefin blends.⁶ The results at different compositions are almost parallel to each other and shift upward with increasing composition asymmetry. Similar findings were obtained at the three different monomer densities considered. To our knowledge, this is the first simulation evidence of a q -dependent value of the SANS-derived interaction parameter. The results at $N = 50$ had much smaller

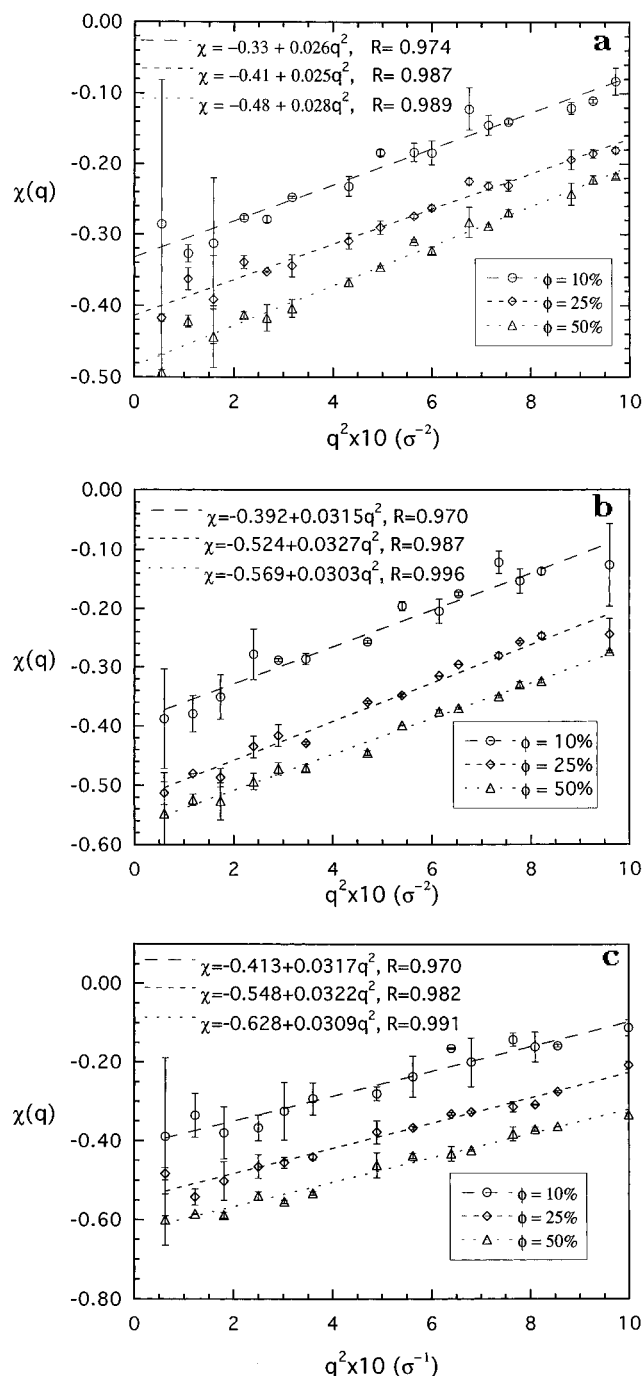


Figure 4. (a) Calculated χ parameter as a function of q^2 for the attractive blend at total monomer density $\rho^* = 0.70$ and three different compositions. The chain lengths for both components are $N = 25$. (b) The same as in part a, except that $\rho^* = 0.80$. (c) The same as in part a, except that $\rho^* = 0.85$.

magnitudes for $\chi(q)$ as expected and, consequently, much larger relative errors.

Figure 5 shows the zero wave-vector χ parameter determined from the above procedure plotted as a function of the volume fraction of component 1. From the figure it is clear that the χ parameter for the $N = 25$ system shows a parabolic dependence on composition. This trend has been reported before from computer simulations.^{17–19} It was suggested in previous work¹⁵ that, while simulations conducted at constant pressure yield composition-independent χ parameters, the χ parameters obtained from simulations at constant density showed a parabolic composition dependence. This result has been attributed to equation of state

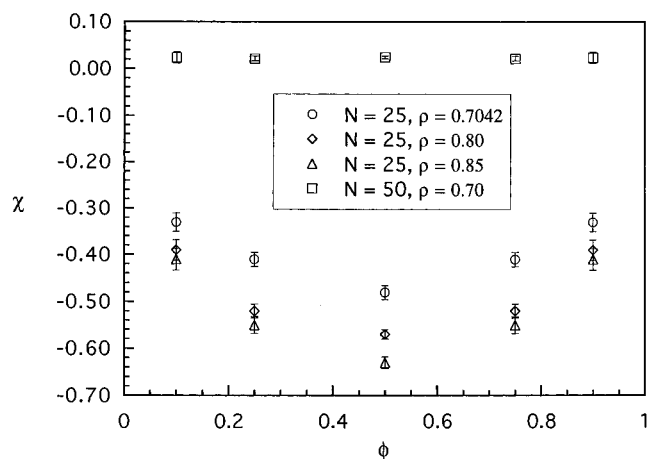


Figure 5. Variation of the zero wave-vector χ parameter as a function of composition for the attractive and repulsive blends. The error bars are obtained from linear regression analysis based on the $\chi(q)$ values in Figure 4.

Table 3. Equation of State Data for the Attractive Systems Studied at Various Total Monomer Densities and Compositions^a

ρ^*	T^*	N	pressure ($P^* = P\sigma^3/\epsilon$)		
			$\phi = 0.10$	$\phi = 0.25$	$\phi = 0.50$
0.70	2.0	25	0.49 (11)	0.39 (11)	0.35 (8)
0.80	2.0	25	1.60 (12)	1.47 (13)	1.43 (13)
0.85	2.0	25	2.59 (13)	2.44 (14)	2.33 (13)

^a The numbers in the parentheses represent the statistical uncertainty. Therefore, 0.49 (11) implies 0.49 ± 0.11 .

effects since the pressure changes with composition under these conditions. Since our simulations are conducted at constant density, we have calculated the pressure in our simulation (using atomic virial for the pressure²⁴), to verify these ideas (see Table 3). As can be seen, the pressure increases systematically as the composition becomes more asymmetric, but the trend is at the limit of our statistical significance. This indicates that at least some of the composition dependence of the χ parameter observed in Figure 5 may be attributable to equation of state effects. Further work needs to be performed at more state conditions to test this idea more fully.

Returning now to Figure 5, we see that for the attractive system, as the total monomer density of the system increases, the calculated χ parameter becomes more negative. This may be understood intuitively as a result of the increase in the number of interactions per unit volume. Also plotted in the figure is the zero wave-vector limit of the χ parameter for the repulsive $N = 50$ system. Because the χ is small in magnitude, these simulation results cannot distinguish whether or not there is composition dependence in the χ parameter, which is small and positive.

3.3. Discussion. There are two separate issues that need to be discussed in some more detail. First, as observed in Figure 4, the calculated χ values for the attractive system show a linear dependence on q^2 . The origins of this behavior need to be understood. Second, we would like to systematically evaluate the role of compressibility on the partial structure factors, as well as the total structure factors of these systems.

In Figure 6 we plot the three different partial structure factors in the form $1/S_{ij}(q)$ vs q^2 for the $N = 25$ system at $T^* = 2$ and $\phi = 0.1$ for two different densities. It is clear that all three structure factors plotted in this

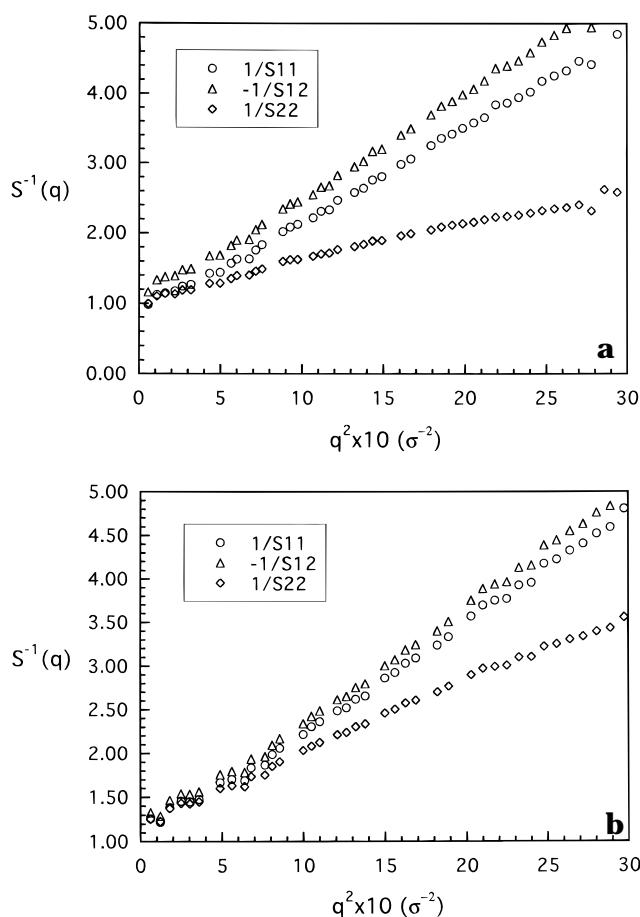


Figure 6. (a) Inverse of the three partial structure factors vs q^2 at $\rho^* = 0.70$ and composition $\phi = 0.10$ of component 1. (b) Same as part a, except for $\rho^* = 0.85$.

form display linear dependences, showing that they follow an Ornstein–Zernike form, i.e.

$$\frac{1}{S(q)} = \frac{1}{S(0)} + Aq^2 \quad (10)$$

where A is a constant. However, the slopes of the three different lines are not identical. This is a somewhat surprising result, since the i-RPA would suggest that $S_{11}(q) = S_{22}(q) = -S_{12}(q)$ for an incompressible system.³ Consequently, it would appear that a consequence of finite compressibility is that, in general, each partial structure factor possesses a different wave-vector dependence.¹⁴ One means to verify this conclusion is to check our results against the prediction of compressible RPA theories, such as the one proposed recently by Tang and Freed,¹⁰ which shows that the three different partial structure factors must have different q -dependences. However, it is difficult to make a quantitative comparison of our off-lattice results to their lattice theory since several quantities, such as the hole fraction, are not easy to identify from our simulations. Consequently, we are forced to conclude that, in a qualitative manner, the presence of compressibility causes the three structure factors to have different q -dependences. At this time, we cannot decide if all of the observed difference in behavior observed in Figure 6 can be explained by this compressibility effect.

An important implication of the results shown in Figure 6, as well as the compressible RPA,¹⁰ is that the combination of the three partial structure factors with different q -dependences into a total structure factor,

Table 4. Estimated Partial Volume per Monomer, $v_i^* = v_i/\sigma^3$, and Isothermal Compressibility, $\rho k_B T \kappa_T$, at Various Compositions for the Attractive Systems of Chain Length $N = 25$ at $T^* = 2$

ρ^*	T^*	$\rho k_B T \kappa_T$			$\phi = 0.10$		$\phi = 0.25$		$\phi = 0.50$	
		$\phi = 0.10$	$\phi = 0.25$	$\phi = 0.50$	v_1^*	v_2^*	v_1^*	v_2^*	v_1^*	v_2^*
0.70	2.0	0.31	0.25	0.28	1.20	1.44	1.27	1.48	1.43	1.43
0.80	2.0	0.07	0.14	0.12	1.16	1.25	1.17	1.27	1.25	1.25
0.85	2.0	0.10	0.07	0.09	1.14	1.19	1.14	1.18	1.18	1.18

^a It is difficult to determine the statistical uncertainties in these quantities.

such as in eq 9, will result in a function with a q -dependence that will not, in general, be described by the i-RPA. Consequently, the χ parameter that is obtained by applying the incompressible eq 2 to results from a compressible system will vary linearly with q^2 , especially at low q . This result can potentially explain the observed q -dependence of the interaction parameters in Figure 5 as well as in published experimental results.⁴

Having outlined the role of compressibility on the q -dependence of the interaction parameter, we now study its consequences on the $q = 0$ limit through a thermodynamic procedure. Through this approach we shall show below that the partial molar volume of the majority component changes very little with the composition and is approximately equal to the molar volume of the mixture. In contrast, the partial molar volume of the minority component in the attractive blend decreases with composition. Consequently, the reason the $q = 0$ limits of the three partial structure factors are different is primarily because the partial molar volumes for the two components are quite different, thus reasserting the importance of compressibility effects in this context. Fluctuation theory shows that the partial structure factors at $q = 0$ follow the thermodynamic identities,^{15,27,28}

$$S_{11}(0) = \rho k_B T \kappa_T \phi_1^2 + \phi_1 \phi_2 (\rho v_2)^2 \left[\frac{\partial(\beta \mu_1 / N_1)}{\partial \ln \phi_1} \right]_{T,P}^{-1} \quad (11a)$$

$$S_{12}(0) = \rho k_B T \kappa_T \phi_1 \phi_2 + \phi_1 \phi_2 \rho^2 v_1 v_2 \left[\frac{\partial(\beta \mu_1 / N_1)}{\partial \ln \phi_2} \right]_{T,P}^{-1} \quad (11b)$$

$$S_{22}(0) = \rho k_B T \kappa_T \phi_2^2 + \phi_1 \phi_2 (\rho v_1)^2 \left[\frac{\partial(\beta \mu_2 / N_2)}{\partial \ln \phi_2} \right]_{T,P}^{-1} \quad (11c)$$

with the additional relation that $S_{12}(0) = S_{21}(0)$. Here ρ is the monomer density, k_B is Boltzmann's constant, T and P are the temperature and pressure, κ_T is the isothermal compressibility of the system, and ϕ_i , v_i , μ_i , and N_i are the composition, partial volume per monomer, segmental chemical potential, and chain length of component i in the binary polymer blend, respectively. Note that the derivatives are taken under the constant temperature and pressure conditions. The first term in each of these equations is the contribution from density fluctuations, while the second term arises from composition fluctuations. Following the Gibbs–Duhem relation, the derivatives in the second term of eqs 11a and 11c are equal and are negative that of the second term of eq 11b. From eqs 11, it is relatively straightforward to show that¹⁴

$$\frac{k_B T \kappa_T}{\rho} = \sum_{ij} v_i v_j S_{ij}(0) \quad (12)$$

For the equal composition case, by definition, $v_1 = v_2 =$

$1/\rho$. Using the extrapolated zero wave-vector values of the partial structure factors, $S_{11}(0) = 1.0$, $S_{22}(0) = 1.0$, and $S_{12}(0) = -0.86$ at $\rho^* = 0.70$ for the attractive $N = 25$ system at $T^* = 2$, eq 12 yields $\rho k_B T \kappa_T \approx 0.28$. Similarly, we obtain $\rho k_B T \kappa_T \approx 0.09$ at $\rho^* = 0.85$. Using $S_{11}(0) \sim 1.0$ and 0.80 , at the two densities respectively, we estimate that the contributions to the scattering due to density fluctuations are about 7% and 3%, respectively, at the two densities.

For the unequal composition, the molar volumes of the two components are, in general, not the same, and a rigorous determination of the isothermal compressibility is more difficult. For the composition $\phi = 0.10$ at $\rho^* = 0.70$, $1/S_{11}(0) = 1.0$, $1/S_{22}(0) = 1.0$, and $1/S_{12}(0) = -1.2$. We assume that the first term in eqs 11a and 11b can be safely neglected due to the presence of the term ϕ_1 . This immediately yields $v_2/v_1 = S_{11}(0)/S_{12}(0) = 1.0/1.2 \approx 0.83$. Solving this equation together with the identity $\phi_1 v_1 + \phi_2 v_2 = 1/\rho$, we obtain $v_1 = 1.20$ and $v_2 = 1.44$. These values of v_1 and v_2 can be substituted in eq 12 to yield $\rho k_B T \kappa_T = 0.31$. This value is very close to the value obtained at $\phi = 0.50$. On the basis of this estimate, we now compute that the ratio of the first term to the second term of eq 11a is 0.3% and that in eq 11b is $0.31/11.1 \sim 3\%$, thus justifying our initial neglect of the density fluctuation term. In a similar manner, we estimated the partial volume per monomer and compressibility for the attractive systems of chain length $N = 25$ at various overall monomer densities and compositions; the results are tabulated in Table 4. It is seen from Table 4 that when the composition of the two components becomes more asymmetric, the overall trend is that the partial volume of the majority component stays constant, while that of the minority component decreases. The variation is much weaker at high overall monomer density. Further note that the compressibility decreases with an increase of the overall monomer density.

Conclusions

By carrying out molecular dynamics simulations for model polymer blend systems consisting of a relatively large number of chains, we computed the three partial structure factors of the blends in the small q limit. At the level of a single chain we found that the polymer molecules assume Gaussian shapes for length scales larger than the monomer size. These results are in good agreement with theoretical expectations. However, chain dimensions of the minority component in the blend change quite significantly on blending, a result that is in good agreement with past simulations. It is found that the three partial structure factors in the blend followed Ornstein–Zernike behavior, but with different slopes and $q = 0$ intercepts. These results are shown to be a consequence of system compressibility, thus illustrating that compressibility effects play a critical role in the small-angle scattering data that is obtained even from these simplest possible classes of polymer mixtures.

Acknowledgment. This work was sponsored by the Laboratory Directed Research and Development Program of ORNL. The work of H.D.C. was supported by the Division of Chemical Sciences of the U.S. Department of Energy. The authors acknowledge the use of the Intel Paragon supercomputers in the Center for Computational Sciences at ORNL, funded by the DOE's Mathematical, Information, and Computational Sciences Division. ORNL is managed by Lockheed Martin Energy Research Corp. for the DOE under Contract No. DE-AC05-96OR22464. Funding for this work at Penn State University was provided by the National Science Foundation under Grant CTS-9311915. Part of this work was performed when S.K.K. was a visitor at ORNL. He acknowledges their kind hospitality.

References and Notes

- (1) See, for example: Lyatskaya, Y.; Gersappe, D.; Gross, N. A.; Balazs, A. C. *J. Phys. Chem.* **1996**, *100*, 1449 and references therein.
- (2) Flory, P. J. *Principles of Polymer Chemistry*; Cornell University Press: Ithaca, NY, 1954. Flory, P. J. *J. Chem. Phys.* **1941**, *9*, 660. Huggins, M. L. *J. Chem. Phys.* **1941**, *9*, 440.
- (3) de Gennes, P.-G. *J. Phys. (Paris)*, **1970**, *31*, 235.
- (4) Brereton, M. G.; Fischer, E. W.; Herkt-Maetzky, C.; Mortensen, K. *J. Chem. Phys.* **1987**, *87*, 6144.
- (5) Bates, F. S.; Muthukumar, M.; Wignall, G. D.; Fetters, L. J. *J. Chem. Phys.* **1988**, *89*, 535.
- (6) Krishnamoorti, R.; Graessley, W. W.; Balsara, N. P.; Lohse, D. J. *J. Chem. Phys.* **1994**, *100*, 3894.
- (7) Londono, J. D.; Narten, A. H.; Wignall, G. D.; Honnell, K. G.; Hsieh, E. T.; Johnson, T. W.; Bates, F. S. *Macromolecules* **1994**, *27*, 2864.
- (8) Muthukumar, M. *J. Chem. Phys.* **1986**, *85*, 4722.
- (9) Olvera de la Cruz, M.; Edwards, S. F.; Sanchez, I. C. *J. Chem. Phys.* **1988**, *89*, 1704.
- (10) Tang, H.; Freed, K. F. *Macromolecules* **1991**, *24*, 958.
- (11) Schweizer, K. S.; Curro, J. G. *J. Chem. Phys.* **1989**, *91*, 5059. Schweizer, K. S.; Curro, J. G. *Phys. Rev. Lett.* **1988**, *60*, 809. Curro, J. G.; Schweizer, K. S. *Macromolecules* **1991**, *24*, 6736.
- (12) Hammouda, B. *J. Non-Cryst. Solids* **1994**, *172-174*, 927.
- (13) Taylor, J. K.; Debenedetti, P. G.; Graessley, W. W.; Kumar, S. K. *Macromolecules* **1996**, *29*, 764.
- (14) Bidkar, U. R.; Sanchez, I. C. *Macromolecules* **1995**, *28*, 3963.
- (15) Kumar, S. K. *Macromolecules* **1994**, *27*, 260.
- (16) Briber, R. M.; Bauer, B. J.; Hammouda, B. *J. Chem. Phys.* **1994**, *101*, 2592.
- (17) Sariban, A.; Binder, K. *J. Chem. Phys.* **1987**, *86*, 5859.
- (18) Sariban, A.; Binder, K. *Macromolecules* **1988**, *21*, 711.
- (19) Sariban, A.; Binder, K. *Colloid Polym. Sci.* **1989**, *267*, 469.
- (20) Cui, S. T.; Cummings, P. T.; Cochran, H. D. *ISUG '96* and *J. Comput. Math.* **1996**, submitted.
- (21) Kremer, K.; Grest, G. S. *J. Chem. Phys.* **1990**, *92*, 5057.
- (22) de Pablo, J. J.; Laso, M.; Suter, U. W. *J. Chem. Phys.* **1992**, *96*, 2395.
- (23) Rouse, P. E. *J. Chem. Phys.* **1953**, *21*, 1272. Doi, M.; Edwards, S. F. *The Theory of Polymer Dynamics*; Oxford University Press: New York, 1986.
- (24) Allen, M. P.; Tildesley, D. T. *Computer Simulation of Liquids*; Oxford University Press: New York, 1987.
- (25) Higgins, J. S.; Benoit, H. C. *Polymers and Neutron Scattering*; Oxford University Press: New York, 1994.
- (26) de Gennes, P.-G. *Scaling Concepts in Polymer Physics*; Cornell University Press: Ithaca, NY, 1979.
- (27) Hill, T. L. *Statistical Mechanics*; McGraw-Hill: New York, 1956.
- (28) Dudowicz, J.; Freed, K. F. *Macromolecules* **1991**, *24*, 5112.

MA961020H